Development of lipidoid nanoparticles for siRNA delivery to neural cells

Purva Khare,[1] Kandarp M. Dave,[1] Yashika S. Kamte,[1] Muthiah A. Manoharan,[2] Lauren A. O'Donnell,[1] Devika S Manickam[1†]

[1]Graduate School of Pharmaceutical Sciences, Duquesne University, Pittsburgh, PA, USA.

[2]Alnylam Pharmaceuticals, Cambridge, MA, USA.

†Corresponding author: Devika S Manickam
453 Mellon Hall, 600 Forbes Avenue,
Pittsburgh, PA 15282.
Email: soundaramanickd@duq.edu
Twitter @manickam_lab
Phone: +1 (412) 396-4722, Fax +1 (412) 396-2501

Abstract

Lipidoid nanoparticles (LNPs) are the delivery platform in Onpattro, the first FDA-approved siRNA drug. LNPs are also the carriers in the Pfizer-BioNTech and Moderna COVID-19 mRNA vaccines. While these applications have demonstrated that LNPs effectively deliver nucleic acids to hepatic and muscle cells, it is unclear if LNPs could be used for delivery of siRNA to neural cells, which are notoriously challenging delivery targets. Therefore, the purpose of this study was to determine if LNPs could efficiently deliver siRNA to neurons. Because of their potential utility in either applications in the central nervous system and the peripheral nervous system, we used both cortical neurons and sensory neurons. We prepared siRNA-LNPs using C12-200, a benchmark ionizable cationic lipidoid along with helper lipids. We demonstrated using dynamic light scattering that the inclusion of both siRNA and PEG-lipid provided a stabilizing effect to the LNP particle diameters and polydispersity indices by minimizing aggregation. We found that siRNA-LNPs were safely tolerated by primary dorsal root ganglion neurons. Flow cytometry analysis revealed that Cy5 siRNA delivered via LNPs into rat primary cortical neurons showed uptake levels similar to Lipofectamine RNAiMAX—the gold standard commercial transfection agent. However, LNPs demonstrated a superior safety profile whereas the Lipofectamine-mediated uptake was concomitant with significant toxicity. Fluorescence microscopy demonstrated a time-dependent increase in the uptake of LNP-delivered Cy5 siRNA in a human cortical neuron cell line. Overall, our results suggest that LNPs are a viable platform that can be optimized for delivery of therapeutic siRNAs to neural cells.

Keywords

Lipidoid nanoparticle, C12-200, siRNA, neural cell, transfection

Introduction

Delivery of small interfering RNA (siRNA) is a promising strategy to treat pathologies as it allows genetic manipulation with a greater degree of target specificity with fewer off-target effects (1, 2). Lipidoid nanoparticles (LNPs) are the carriers in Onpattro, the first LNP-based RNAi drug to gain FDA approval for the treatment of polyneuropathies caused by a rare and life-threatening disorder, hereditary transthyretin-mediated amyloidosis (3). The clinical utility of LNPs is further reiterated by the recent emergency approvals of COVID-19 mRNA vaccines by Pfizer-BioNTech and Moderna (4). Based on the clinical success of LNPs in delivering siRNAs to hepatic and non-hepatic targets (7–9), we explored if LNPs could effectively deliver siRNA to neural cells. Neural cells are targets for drug delivery in multiple CNS disorders such as Alzheimer's disease, Parkinson's disease, ischemic stroke, peripheral nerve injuries, neuropathic and inflammatory pain (8–12). The key challenge associated with the delivery of siRNA to neural cells are its poor accumulation and short duration of action inside cells.

The potent delivery characteristics of LNPs may allow them to be optimized for neural cell delivery. LNPs are primarily composed of an ionizable cationic lipidoid along with helper lipids like distearylphosphatidylcholine (DSPC), polyethylene glycol-dimyristoyl glycerol (PEG-DMG) and cholesterol (13, 14). Ionizable cationic lipidoids allow higher encapsulation efficiencies and greater intracellular release via effective endosomal escape (15). Ionizable cationic lipidoids with pKa values between 6-7 acquire a positive charge at acidic pH and result in electrostatic interactions with the negatively charged siRNA molecules leading to the spontaneous formation

of LNPs. At physiological pH of 7-7.4, these obtain a neutral charge and thereby largely eliminate the toxicity associated with cationic lipids such as lipofectamine (16). This key feature renders the LNPs a superior safety profile compared to cationic transfection agents. The acidic microenvironment of endosomes lend the LNPs a positive charge because of which they associate with negative anionic endosomal lipids leading to endosomal destabilization and improved siRNA release into the cytoplasm (17, 18).

Seminal studies by Langer, Anderson and colleagues developed high throughput lipidoid libraries consisting of thousands of ionizable cationic lipidoids and identified lead lipidoids based on their *in vitro* and *in vivo* delivery efficacies in rodents as well as non-human primates. Amongst those, C12-200 lipidoid demonstrated the highest knockdown and uptake *in vitro* (7, 19, 20). Therefore, we chose C12-200 lipidoid as the ionizable cationic lipidoid component of LNPs. LNP-based siRNA delivery harnesses several key advantages of LNP chemistry such as high transfection efficiency, low toxicity and immunogenicity, protection of the payload from physiological enzymes to increase their metabolic stability, ability for ligand conjugation and enhancing the overall pharmacokinetics of the delivered cargo (21–23). The novelty of our work lies in exploiting some of these cardinal features of LNPs to maximize siRNA uptake into neural cells, a notoriously challenging delivery target.

In this pilot study, we formulated siRNA-LNPs using C12-200 lipidoid and characterized their colloidal stability using dynamic light scattering. We characterized their cytocompatibility with a panel of breast cancer cell lines and a model of sensory neurons, primary dorsal root ganglion cultures. We studied the qualitative and quantitative uptake of siRNA delivered via LNPs into

neurons using fluorescence microcopy and flow cytometry, respectively. Despite mediating similar levels of siRNA uptake, we found that LNPs are a safe carrier and show no signs of toxicity in the neuronal models compared to the commercially available cationic lipid, Lipofectamine. These findings encourage the further optimization of LNPs for knockdown of therapeutically-relevant neuronal targets.

Experimental section

Materials

1,2-distearoyl-sn-glycero-3-phosphocholine (DSPC) (850365P) and 1,2-Dimyristoyl-rac–glycero-3-methoxypolyethylene glycol-2000 (PEG-DMG) (8801518) were obtained from Avanti Polar Lipids (Alabaster, AL). Cholesterol (8667) and Cy5-labeled siRNA were procured from Sigma-Aldrich (St. Louis, MO). 1,1‘-((2-(4-(2-((2-(bis (2 hydroxy dodecyl) amino) ethyl) (2hydroxydodecyl) amino) ethyl) piperazin1yl) ethyl) azanediyl) bis(dodecan-2-ol) (C12-200), an ionizable cationic lipidoid was a generous gift from Alnylam Pharmaceuticals (Cambridge, MA). Quant-iT Ribogreen RNA Assay Kit (R11490) was purchased from Life Technologies (Carlsbad, CA). Triton X-100 was procured from Acros organics (Morris Plains, NJ). Heat-inactivated fetal bovine serum (FBS) and phosphate buffered saline (PBS) were purchased from Hyclone Laboratories (Logan, UT). TrypLE express, RPMI + GlutaMAX-I (1X) and DMEM/F-12 were purchased from Life Technologies Corporation (Grand Island, NY). MCF-7, MDA-MB-231 and BT-549 cell lines were generously provided by Dr. Jane Cavanaugh (Duquesne University). Human cortical neuron cell line (HCN-2) (CRL-10742) and primary rat cortical neurons (RCN) (A10840-02) were purchased from ATCC (Manassas, VA) and Thermo Fisher Scientific (Frederick, MD) respectively. siGAPDH (Silencer Select GAPDH siRNA), siTRPV1 (5'

GCGCAUCUUCUACUUCAACTT 3', 3' TTCGCGUAGAAGAUGAAGUUG 5') and control, inverted siTRPV1 (5' CAACUUCAUCUUCUACGCGTT 3', 3' TTGUUGAAGUAGAAGAUGCGC 5') were procured from Thermo Fisher Scientific (Austin, TX). All reagents were used as received unless stated otherwise.

Preparation of siRNA-loaded LNPs (siRNA-LNPs)

LNPs were prepared using previously reported methods (7). Briefly, the ionizable cationic lipidoid C12-200, DSPC, cholesterol and PEG-DMG were dissolved in ethanol at a molar ratio of 50/10/38.5/1.5. A one mg/mL solution of siRNA was prepared in 10 mM citrate buffer, pH 4.0. The solutions were mixed immediately for the 'slow mixing' and for the 'fast mixing' protocol, the lipid phase was added dropwise to the aqueous phase under continuous vortexing for 30 seconds while maintaining the Fisher benchtop vortexer knob at position 7. The LNPs were then allowed to stand for ten minutes. A precalculated volume of 1*X* PBS pH 7.4 was then added to the LNPs to adjust the final siRNA concentration to 400 nM. All the formulations were made at a final siRNA concentration of 400 nM and cationic ionizable lipidoid/siRNA w/w ratio was maintained at 5:1, unless stated otherwise.

Agarose gel electrophoresis

Agarose gel electrophoresis was performed to qualitatively confirm the encapsulation of siRNA in LNPs. Briefly, a 2% agarose gel was prepared in 1*X* Tris-borate buffer composed of 108 g Tris and 55 g Boric acid dissolved in 900 ml distilled water with 40 ml of 0.5 M Na_2EDTA and 0.05% Ethidium bromide. Samples pre-mixed with 1*X* RNA loading buffer were electrophoresed in an Owl EasyCast B2 Mini Gel Electrophoresis System (Thermo Fisher Scientific, St. Louis, MO) for

90 min. The gel was imaged under UV light using a Gel Doc system (ProteinSimple, San Jose, CA).

Determination of the extent of siRNA loading using the RiboGreen assay

The extent of siRNA loading in the prepared LNPs was measured using the Quant-iT Ribogreen RNA Assay Kit by following the manufacturer's instructions. RiboGreen is a fluorescent dye, which, in its free form exhibits minimal fluorescence but when bound to a nucleic acid, it fluoresces with an exceptionally high intensity that is directly proportional to the amount of nucleic acid (24). Total siRNA content is defined as the amount of encapsulated and non-encapsulated/free siRNA in the LNPs. The difference between the total and free siRNA was used to calculate the amount of siRNA encapsulated within the LNPs. A fresh sample of two µg/mL dsRNA stock solution was prepared each time with 1*X* Tris-EDTA (TE) and the standard curve was generated at concentrations ranging from 0-1000 ng/mL. A free siRNA sample was prepared with 1*X* TE and LNPs were lysed with 2% Triton X-100 in 1*X* TE to measure the "total" siRNA content. The fluorescence intensities were measured on a SYNERGY HTX multi-mode reader (Winooski, VT) at an excitation wavelength of 485 nm and an emission wavelength of 528 nm. The % encapsulation efficiency was calculated using the **Eq. 1**.

$$\%\ siRNA\ encapsulation\ efficiency = \frac{(Amount\ of\ total\ siRNA\ in\ the\ sample - Amount\ of\ free\ siRNA\ in\ the\ sample)}{Amount\ of\ total\ siRNA\ in\ the\ sample} \times 100\% \quad \textbf{Equation 1}$$

Dynamic Light Scattering

To determine the physical stability of LNPs, the average particle diameters, polydispersity indices and zeta potentials of the blank and siGFP-loaded LNPs were measured by dynamic light

scattering (DLS) using a Malvern Zetasizer Pro (Malvern Panalytical Inc., Westborough, PA) over a period of seven days with intermittent storage at 2-8°C. The prepared LNPs were diluted to a siRNA concentration of 40 nM using 10 mM 1*X* PBS pH 7.4 for particle size measurements and using deionized water for zeta potential measurements. All measurements were carried out in triplicate and the data are presented as average + standard deviation (SD) and are representative of at least five-six independent experiments (measurement errors <5%).

Cell culture

MCF-7 and BT-549 cells were maintained in RPMI + GlutaMAX (1*X*) supplemented with 10% FBS. MDA-MB-231 cells were maintained in DMEM/F-12 1:1 medium supplemented with 2.5 mM L-Glutamine + 15 mM HEPES Buffer + 110 mg/L Sodium Pyruvate + 10% FBS. The growth medium was changed every 48 hours. Primary rat dorsal root ganglion (DRG) cultures were isolated using previously reported methods (25). DRG cultures were maintained in DMEM/high glucose (4.5 g/L glucose) media supplemented with 2.5 mM L-Glutamine + 15 mM HEPES Buffer + 110 mg/L Sodium Pyruvate + 10 % FBS. Human cortical neuron cell line was maintained in DMEM/high Glucose (4.5 g/L glucose) medium supplemented with 10 % FBS. Primary rat cortical neurons were maintained in Neurobasal Plus medium supplemented with 200 mM GlutaMAX I and B-27 Plus supplement. All cultures were maintained in a humidified incubator at 37 ^{o}C and 5% CO_2.

Cytocompatibility of LNPs

MCF-7, MDA-MB-231, BT-549 cells and primary rat DRG neurons were seeded in a clear, flat bottom Poly-D-Lysine coated 96-well plate (Azer Scientific, Morgantown, PA) for the

cytocompatibility studies. MCF-7, MDA-MB-231, BT-549 cells were seeded at a density of 5,000 cells/well and DRG neurons were seeded at a density of 1,500 cells/well. Untreated cells were used as a control in all studies. Cells were transfected for 4 h with LNPs containing 50 nM of siRNA in complete growth medium in a volume of 50 μL/well. Post-transfection, the transfection mixture was replaced with 200 μL of fresh complete growth medium/well followed by a 24-hour incubation at 37°C and 5% CO_2. The relative intracellular ATP levels were measured using the Cell Titer-Glo luminescence assay (ATP assay) 24 h-post transfection using previously described methods (26–28). The levels of ATP directly correlate with the cell numbers used here as a measure of cell viability. The ATP levels of the treatment groups were measured against those of the untreated or control cells. Briefly, 60 μL of the complete growth media and 60 μL of Cell Titer Glo 2.0 reagent were added to each well of the 96-well plate. The plate was incubated for 15 minutes in dark at room temperature in an incubator-shaker (Thermo Fisher Scientific, Waltham, MA). Following incubation, 60 μL of the mixture from each well was transferred to a flat-bottom, white opaque 96-well plate (Azer Scientific, Morgantown, PA). The luminescence was measured using SYNERGY HTX multi-mode reader (BioTek Instruments, Winooski, VT). Relative ATP levels (%) were calculated for the transfection groups by normalizing them to the luminescence of the untreated cells as shown in **Eq.2**.

$$\text{Relative ATP levels (\%)} = \frac{Luminescence\ from\ cells\ treated\ with\ samples}{Luminescence\ from\ untreated\ cells} \times 100 \qquad \textbf{Equation 2}$$

Cy5 siRNA uptake into primary rat cortical neurons using flow cytometry

Neurons were plated in a clear, flat-bottom Poly-D-Lysine coated 24-well plate (Genesee Scientific, San Diego, CA) at a density of 50,000 neurons/well in Complete Neurobasal Plus media and were allowed to acclimatize at 37°C and 5 % CO_2 for 4-5 days. Cy5 siRNA containing LNPs

were prepared as described earlier and diluted with the Complete Neurobasal Plus to a final Cy5 siRNA concentration of 50 nM. The neurons were incubated with the transfection mixture for 24 h. The transfection mixture contained either naked Cy5 siRNA or Cy5 siRNA-LNPs with PEG-DMG (+ PEG-DMG) or Cy5 siRNA-LNPs without PEG-DMG (- PEG-DMG) or Cy5 siRNA-Lipofectamine RNAiMAX complexes. Post-exposure, cells were gently removed from the wells and collected in microcentrifuge tubes. The cell suspension was centrifuged at 300 g for 5 minutes and the pellet was resuspended in 500 µL *1X* PBS. Cells were then analyzed using Attune NxT Acoustic Focusing Cytometer (Singapore) equipped with Attune NxT software. The fluorescence intensity of Cy5 siRNA was detected at an excitation wavelength of 638 nm and an emission wavelength of 720/30 nm. A total of 30,000 events were recorded for each sample. Histogram plots were obtained from the Attune NxT software. Cells were gated using forward vs. side scatter plots to exclude dead cells and cell debris. Untreated cells were used as negative-staining controls to set a gate for Cy5-negative and Cy5-positive populations. Data are presented as a percentage of Cy5-positive (Cy5 (+)) events.

Cy5 siRNA uptake by fluorescence microscopy in a human cortical neuron cell line

We used fluorescence microscopy to determine the Cy5 siRNA uptake into a neuronal cell line. Human cortical neurons (HCN-2) were seeded in a clear, flat-bottom, Poly-D-Lysine coated 48-well plate (Genesee Scientific, San Diego, CA) at a density of 7,000 cells/well. The cells were cultured in complete growth medium in a humidified incubator at 37°C and 5 % CO_2 for 1-2 weeks while replenishing the growth medium every other day. After 4-5 days of culturing, the media was replaced with 175 µL of the transfection mixture. The transfection mixture consisted of either Cy5 siRNA-LNPs or Cy5 siRNA-Lipofectamine RNAiMAX complexes containing 50 nM or 100 nM

of Cy5 siRNA or naked Cy5 siRNA diluted in complete growth media. Cells were incubated with the transfection mixture for two, four and 24 hours at 37°C and 5% CO_2. After the respective time points, the cells were washed once using pre-warmed PBS before adding 0.5 mL of the complete, phenol red-free growth medium/well. Untreated cells and cells treated with Cy5 siRNA-Lipofectamine RNAiMAX complexes were used as negative and positive controls, respectively. Cells were imaged using an Olympus IX 73 epifluorescent inverted microscope (Olympus, Center Valley, PA) to detect Cy5 signals at excitation and emission wavelengths of 651 nm and 670 nm, respectively.

Results

Determination of the extent of siRNA loading using the RiboGreen assay

We used the Ribogreen assay as a quantitative measure to determine the extent of siRNA encapsulation within the LNPs *(Figure 1)* and used agarose gel electrophoresis as a qualitative tool to confirm the absence of 'free' or unentrapped siRNA (*Supplementary Figure 1*). Triton X-100 was used to lyse the LNPs resulting in the extraction of the entrapped siRNA to measure the 'total' siRNA (Total siRNA = entrapped siRNA + free siRNA). Fluorescence readout from LNPs not treated with

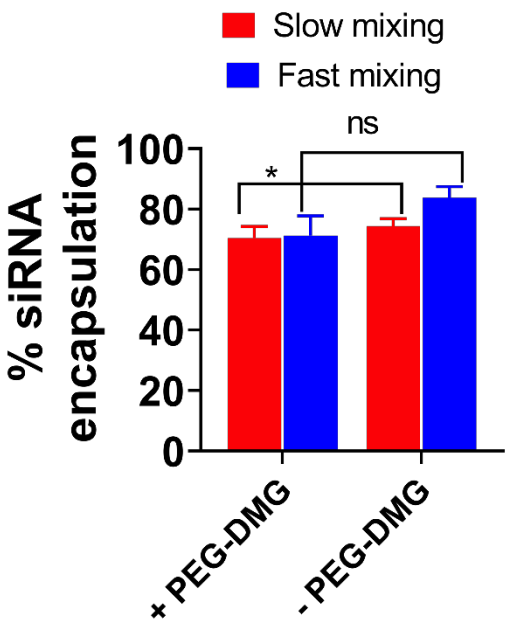

Figure 1. **Extent of siRNA encapsulation in LNPs prepared at different mixing speeds determined by the Ribogreen assay**. The extent of siRNA encapsulation in LNPs (+/- PEG-DMG) was calculated using the following equation ($\frac{(Amount\ of\ total\ siRNA\ in\ the\ sample - Amount\ of\ free\ siRNA\ in\ the\ sample)}{Amount\ of\ total\ siRNA\ in\ the\ sample} \times 100\%$). SiRNA-LNPs were initially prepared in 10 mM citrate buffer and further diluted to a final siRNA concentration of 50 nM using 1*x* PBS. Data are presented as mean ± SD of n=3 samples. Statistical comparisons were made using two-way ANOVA. *$p < 0.05$ and ns: non-significant.

Triton X-100 is indicative of the amount of free siRNA. Two different mixing speeds used during LNP formulation, slow *vs*. fast, were compared for determining their effects on % siRNA encapsulation. The values increased from 74.4% at slow mixing to 83.8% at faster mixing speeds for LNPs prepared without the inclusion of PEG-DMG, whereas we did not observe a significant increase in siRNA loading for LNPs prepared with PEG-DMG at the different mixing speeds.

Colloidal stability of siRNA-loaded LNPs

Physicochemical characteristics of nanocarriers such as particle diameter, polydispersity index (PDI) and surface charge (zeta potential) are influential determinants of their biological activity (29–31). Published studies have reported significant effects of physicochemical characteristics of nano-sized systems on the overall delivery efficacy (32–35). Particle characteristics of self-assembled systems such as LNPs can vary over time during storage potentially affecting their biological activity. We also anticipated that neural cells may show a slower rate of particle uptake compared to non-neuronal cells owing to limited endocytosis/other uptake pathways. We therefore measured the changes in particle diameters and zeta potentials of the LNPs over a period of seven days where the samples were refrigerated interim. Surface coating of nanoparticles using PEG-DMG has been reported to improve their pharmacokinetic profile by reducing the recognition by the mononuclear phagocyte system (36–38). We studied the effect of PEG-DMG in stabilizing LNPs by comparing LNPs prepared in the presence (+) and absence (-) of PEG-DMG. We

compared the particle parameters of blank LNPs and siRNA-loaded LNPs to study the effect of siRNA encapsulation on the resulting particle characteristics.

Blank LNPs (+PEG-DMG) showed average particle diameters of about 250 nm which increased to about 350 nm on day seven. In contrast, the diameters of LNPs (-PEG-DMG) were about 900 nm post-preparation and increased to 4 µm after seven days *(Figure 2a)*. A similar trend was observed for the PDI values of blank LNPs i.e., an initial PDI of 0.32 increased to 0.4 after seven days for LNPs (+PEG-DMG) and an initial PDI of 0.5 increased to 1.8 after seven days for LNPs (-PEG-DMG) (*Figure 2b*). We observed a few statistically significant changes in the particle diameters, PDI values and zeta potential of the prepared LNPs over the period of 7-days *(Supplementary Table 1)*. The narrow polydispersity indices and smaller average particle diameters demonstrate the stabilizing effect of PEG-DMG in the LNPs. siGFP-loaded LNPs (with PEG-DMG) showed average particle diameters of about 120 nm which increased to about 200 nm on day seven (*Figure 2a*). Their initial PDI values of ca. 0.2 increased to about 0.3 after seven days (*Figure 2b*). From this observation we can infer that siRNA loading in the LNPs results in an

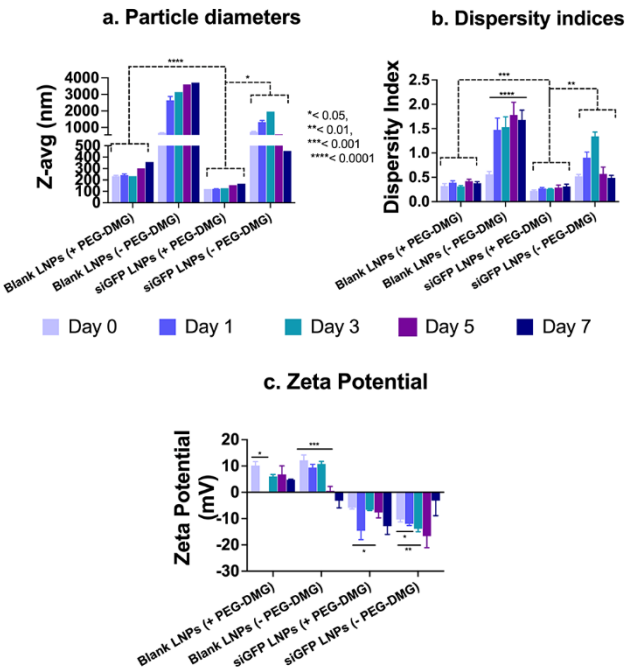

Figure 2. **Colloidal stability of blank or siGFP-loaded LNPs measured using dynamic light scattering**. SiGFP-LNPs were initially prepared in 10 mM citrate buffer and further diluted to a final siRNA concentration of 50 nM using 1*x* PBS. The samples were stored at 2-8 ºC while not in use. Z-average particle diameters (**a**), polydispersity indices (**b**) and zeta potentials (**c**) were measured on a Malvern Zetasizer Pro. Data are presented as mean ± SD of n=3 measurements. Statistical comparisons were made using one-way ANOVA or One sample *t* and Wilcoxon tests. *$p < 0.05$, **$p < 0.01$, ***$p < 0.001$ and ****$p < 0.0001$.

additional stabilizing effect to the respective blank LNP counterparts resulting in narrow and consistent PDI values and particle diameters.

The cationic lipidoid, C12-200, in the LNPs resulted in a net positive charge to the blank LNPs. Blank LNPs containing PEG-DMG showed slightly lower zeta values (6-10 mV) compared to blank LNPs without PEG-DMG (9-12 mV) (*Figure 2c*) that is likely explained by the insertion of PEG chains in between the C12-200 lipidoids or due to formation of a PEG monolayer around C12-200 (39). As seen from *Figure 2c*, siGFP-loaded LNPs showed a negative zeta potential compared to their blank LNP counterparts. Although the changes were not statistically significant, the zeta potentials of the siGFP-loaded LNPs decreased over the seven-day period from -5.91 mV to -19.12 mV. Overall, the average particle diameters and polydispersity indices do not vary significantly over a period of seven days. However, zeta potential values of siGFP-LNPs decreased over a period of seven days. Despite the apparent numerical differences in the zeta potentials, a one-way ANOVA analysis revealed that the differences were not significant.

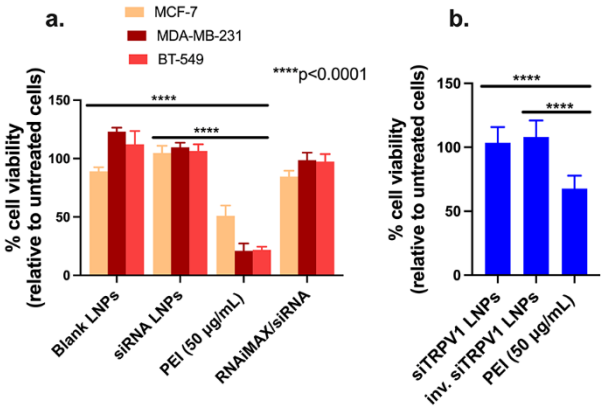

Figure 3. C12-200 LNPs are cytocompatible with TRPV1-expressing breast cancer cell line panel (a) and rat primary DRG neurons (b). Cells were incubated with LNPs containing 50 nM siGAPDH (**a**) and 50 nM siTRPV1 (**b**) for four hours. Untreated cells and cells treated with PEI (50 µg/mL) were used as negative and positive controls, respectively. Cell viability was determined 24 h-post transfection using a CellGlo luminescence viability assay and the data were normalized to untreated cells. Data represents mean + SD (n=6).

Cytocompatibility of C12-200-LNPs

We studied the cytocompatibility of the prepared C12-200/siGAPDH LNPs with MCF-7, MDA-MB-231 and BT-549 cells as these cell models are known to overexpress TRPV1, a neuronal target for siRNA delivery (40). We also studied the compatibility of C12-200/siTRPV1

LNPs with primary rat dorsal root ganglion (DRG) neurons (*Figure 3*). We specifically chose primary rat DRG neurons due to their high expression of TRPV1 (41, 42). TRPV1 is reported to be expressed in 60% of the peripheral nociceptors present in the DRG (43) and is a potential neuronal target for gene knockdown. Cell Titer Glo assay (referred henceforth as the ATP assay) was used the study cytocompatibility of LNPs. The ATP assay is a simple and straightforward technique wherein the readout in relative luminescence units (RLU) can be directly correlated with the ATP levels in the cells. RLU of the untreated cells were normalized to 100% cell viability. Untreated cells and cells treated with a synthetic polycation, polyethyleneimine (PEI) served as the negative and positive controls, respectively. As we expected, MCF-7, MDA-MB-231, BT-549 cells and primary DRG neurons treated with PEI (50 μg/mL), a synthetic polycation known to induce apoptosis showed a 50-60% reduction in cell viability. However, MCF-7, MDA-MB-231 and BT-549 incubated with C12-200/siGAPDH LNPs showed very little evidence of cell death, with cell viabilities >95% 24 h-post transfection. Similarly, siTRPV1-loaded C12-200 LNPs were well tolerated (cell viabilities of ca. 100%) by primary DRG neurons.

Flow cytometry analysis of Cy5 siRNA uptake into primary rat cortical neurons

After confirming that LNPs had little-to-no effect on cell viability, we next wanted to determine if LNPs were taken up by neurons. Because of their commercial availability as well as their non-mitotic nature similar to that of the primary rat DRG neurons, primary rat cortical neurons were used to quantify the uptake levels of Cy5 siRNA using flow cytometry. Lipofectamine RNAiMAX, a cationic lipid, was used as a positive control. Flow cytometry is a quantitative tool for single-cell analysis to measure the light scattered and the fluorescence emitted form a single cell (44). The dead cells/debris were likely removed at the centrifugation step during

the sample processing and as a result, we did not observe any dead cells or debris *(Figure 4a, left)* that are typically found at the bottom left corner of the SSC-A vs. FSC-A plot (45). We then analyzed whether the cells were present in a monodisperse cell suspension to allow for single cell analysis. The forward scatter distributions for height *vs*. area (FSC-A v/s FSC-H) showed a linear profile for about 92% of the recorded events which indicated a single-cell suspension *(Figure 4a, right)*. We analyzed untreated cells and gated out the auto fluorescence *(Figure 4b, left)*. Thus, a shift of signal to the right of the histogram gate (R1 region) was considered to signify that the cell was Cy5-positive (+). The proportion of Cy5 (+) cells directly correspond to the % uptake of Cy5 siRNA in the neurons as represented by the individual histogram plots for the different groups *(Figure 4c)*.

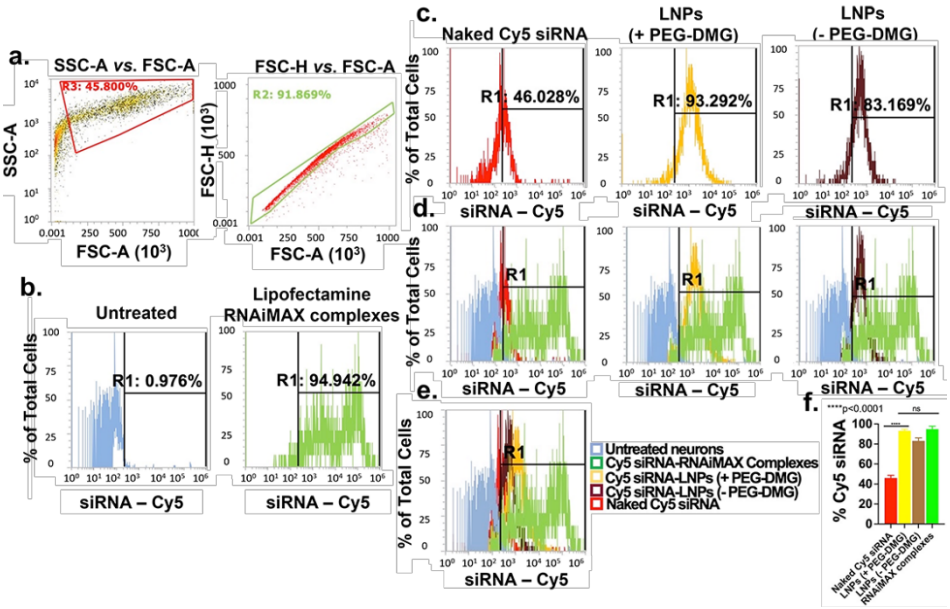

Figure 4. **Uptake of LNPs into rat primary cortical neurons determined using flow cytometry analysis**. Cells were transfected for 24 h with the indicated samples in a 24-well plate. Cy5 siRNA-Lipofectamine RNAiMAX complexes and untreated cells were used as positive and negative controls, respectively. Data are presented as percentages of positive cells for Cy5 (Cy5 (+)). SSC-A *vs*. FSC-A and FSC-H *vs*. FSC-A plots of untreated cells demonstrating monodispersed cells. (**a**), Untreated and Cy5 siRNA/Lipofectamine RNAiMAX-treated cells (**b**), Cells treated with the indicated samples (**c**), Overlay histograms comparing Cy5 (+) cells in each treatment group in comparison to the controls (**d**), Overlay histograms (**e**) and % Cy5 siRNA uptake by the neurons for the respective groups (**f**). The histograms are representative of quadruplicate samples. Statistical comparisons were made using one-way ANOVA. ****$p < 0.0001$.

We then analyzed the % uptake of Cy5 siRNA encapsulated in LNPs prepared with (+) and without (-) the inclusion of PEG-DMG. Around 92-94% *(Figure 4c (yellow))* and 81-83% *(Figure 4c (brown))* cells were Cy5

(+) when transfected with Cy5 siRNA-LNPs prepared with and without the inclusion of PEG-DMG, respectively. *Figure 4d* shows the relative Cy5+ cells in each of the indicated groups in reference to the untreated (blue) and positive control-treated (green) groups. The rightward shift in intensities of Cy5 (+) cells for all the groups in comparison with the controls are demonstrated in the overlay histogram plot in *Figure 4e.* As expected, the % uptake of Cy5 siRNA was least in cells treated with free Cy5 siRNA and greatest in cells treated with LNPs (+PEG-DEMG) and Cy5 siRNA/Lipofectamine RNAiMAX complexes (*Figure 4e and f)*. Furthermore, as seen in *Figure 4e*, we saw a greater uptake of LNPs with PEG-DMG as compared to those without PEG-DMG. Particle sizes of LNPs play one of the major roles in determining uptake levels and therefore, lower diameter particles may allow efficient cellular internalization. Furthermore, a significant difference in the uptake of Cy5 siRNA was observed when transfected with naked Cy5 siRNA and Cy5 siRNA-LNPs (+/- PEG-DMG) *(*Figure 4*e and f)*. This reiterates the need for a safe and efficient transfection agent to maximize the uptake of siRNA in neurons, a hard-to-transfect cell type.

Around 94-96% of the cells were Cy5 (+) for the Lipofectamine RNAiMAX group indicating efficient uptake *(Figure 4b right and f)*. Charge-based interactions of cationic lipids with negatively-charged cells allows for higher uptake as compared to neutral or negatively-charged particles. About 44-46% of the cells were Cy5 (+) for the naked Cy5 siRNA transfection group *(Figure 4c (red))*. The difference between the uptake mediated by LNPs (+ PEG-DMG) and Lipofectamine RNAiMAX was statistically non-significant *(Figure 4f)*. Despite the similar levels of uptake among the LNP(+PEG-DMG) and lipofectamine groups, it must also be pointed out that the uptake mediated by Lipofectamine RNAiMAX was accompanied with noticeable cell

stress/toxicity upon visual observation under a microscope whereas LNPs showed a superior safety profile.

Cy5 siRNA uptake by fluorescent microscopy in a human cortical neuron cell line

We studied the effect of exposure time on the uptake of LNPs by incubating the cells for two, four or 24 hours. PEGylation is known to regulate the uptake kinetics of LNPs into cells (46). We compared the differences in uptake for LNPs prepared with/without PEG-DMG. Although Lipofectamine RNAiMAX is a gold standard transfection agent for RNA molecules, it is also quite toxic to cells owing to its strong cationic nature. Therefore, it was unsurprising when we saw changes in morphology indicating cell death, just 2 h after Lipofectamine RNAiMAX was added to cortical neurons, while untreated cells continued to appear spindle-shaped and healthy *(Figure 5a)*.

For this experiment, cells were incubated either with naked Cy5 siRNA, Cy5 siRNA LNP with PEG-DMG, with Cy5 siRNA LNP without PEG-DMG, with Lipofectamine RNAiMAX Cy5 siRNA, or were left untreated. We qualitatively compared the fluorescence intensity among the cells treated with the above samples. Cells treated with naked Cy5 siRNA showed less intense fluorescent signals as compared to cells treated with Cy5 siRNA-LNPs (+/- PEG-DMG) for the two- and four-hour incubation time points *(Figure 5a, b)*. However, we saw a noticeable increase in siRNA uptake 24 h-post transfection (*Figure 5c*). The next pivotal observation was the difference in uptake from the LNPs (+/- PEG-DMG) groups. As mentioned earlier, PEG-DMG plays a key role in determining the physical stability of LNPs as it allows to maintain lower particle diameters by inhibiting particle aggregation (37). We also noted time-dependent differences in

Cy5 siRNA uptake for the LNPs formulated with and without PEG-DMG. LNPs formulated with PEG-DMG showed a time-dependent increase in the uptake of Cy5 siRNA as opposed to LNPs without PEG-DMG where the extent of uptake was not time-dependent. We observed that only a few cells did not show Cy5 siRNA signals when treated with Cy5 siRNA-LNPs (+ PEG-DMG) two- and four-hours post-transfection whereas 24 h post-treatment almost all the cells showed signals corresponding to Cy5 siRNA. Conversely, cells treated with Cy5 siRNA-LNPs (- PEG-DMG) showed efficient uptake of Cy5 siRNA post two- and four hours transfection.

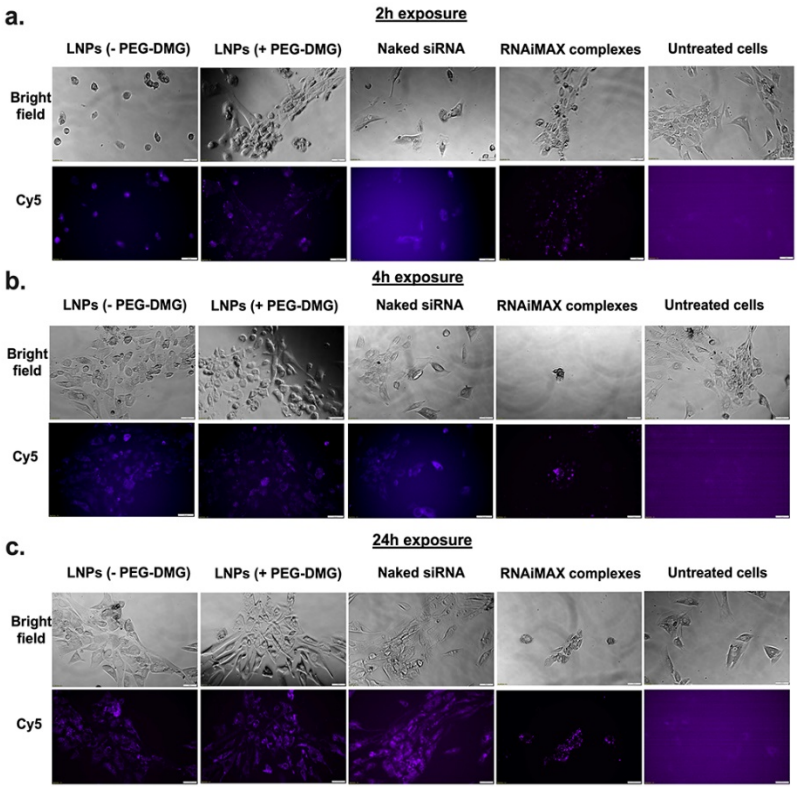

Figure 5. Cellular uptake of Cy5 siRNA determined using fluorescent microscopy. HCN-2 cells (human cortical neuron cell line) were incubated for 2 hours (**a**) 4 hours (**b**) and 24 hours (**c**) with the indicated samples containing 50 nM Cy5 siRNA. Scale bar = 50 µm. Cells were imaged using an Olympus IX 73 epifluorescent inverted microscope to detect Cy5 signals at excitation and emission wavelengths of 651 nm and 670 nm, respectively. Images are representative of n=3 independent wells.

Discussion

The goal of this pilot study was to determine if LNPs based on the benchmark C12-200 lipidoid can be used for siRNA transfection into neurons, a notoriously challenging yet clinically unmet/interesting delivery target. We propose that the well-documented delivery advantages of LNPs including their high levels of siRNA encapsulation, favorable pharmacokinetics, limited immune activation, uptake into target cells and efficient endosomal escape for siRNA into the cytoplasm (14, 47, 48) make them interesting candidates for neural delivery applications.

In this pilot study, we prepared and characterized C12-200 LNPs using DLS. The RiboGreen assay is a well-validated quantitative method to determine the % siRNA loading in LNPs (49, 50). Encapsulation of siRNA in the LNPs for the slow and fast mixing (without PEG-DMG) speeds were about 74.4% and 83.8%, respectively. LNPs with and without PEG-DMG (for fast mixing speed) showed encapsulation efficiencies of about 71.4 % and 83.8 %, respectively *(Figure 1)* which were comparable to the entrapment of siRNA reported for some of the top LNP candidates (51). Although we did not find a significant difference in the encapsulation efficiencies of LNPs prepared with and without PEG-DMG, the inclusion of PEG-DMG serves other vital roles *i.e.*, maintaining lower particle diameters by inhibiting particle aggregation and providing a stealth effect for longer circulation times *in vivo* (37, 38). We further studied the physicochemical stability of the prepared LNPs and compared the stabilizing effect provided by the inclusion of PEG-DMG and siRNA in the LNPs. We utilized siGFP as the model siRNA to compare the siRNA-loaded and blank LNP counterparts prepared both with and without PEG-DMG. We observed a non-significant increase or change in the particle diameters, polydispersity indices and zeta potential over a one-week storage period at 2-8 °C for all the samples *(Figure 2)*. Nevertheless, the particle

diameters differed significantly for blank *vs*. siRNA-loaded LNPs and LNPs with *vs*. LNPs without PEG-DMG *(Figure 2a)*. A similar trend was also observed for the polydispersity indices of blank and siRNA-loaded LNPs; both with and without PEG-DMG *(Figure 2b)*. Our data demonstrated that both siRNA loading and PEG-DMG provided a stabilizing effect to the LNPs by maintaining lower particle diameters and uniform dispersity indices over a period of seven-days.

Although LNPs are deemed to be safe and are well-tolerated by most of the cells, determining their safety and tolerability in neural cells was our primary aim. As shown in *Figure 3*, LNPs were deemed to be well-tolerated by primary DRG neurons as evident by >95% cell viabilities. Establishing the safety profile of LNPs with neural cells allowed further evaluation of their uptake in neural cell lines. We studied the uptake of Cy5 siRNA-loaded LNPs in primary rat cortical neurons and a human neuronal cell line using flow cytometry and fluorescence microscopy, respectively. Previously, Howard *et al* and Thiramanas *et al.* studied the cellular uptake of Cy5 siRNA using flow cytometry (52, 53). As PEG-DMG is known to stabilize the LNPs with resulting lower particle diameters and thus have an impact on their cellular uptake, we compared LNPs prepared with (+) and without (-) PEG-DMG. We used the siRNA complexes of the cationic transfection agent, Lipofectamine RNAiMAX, as a positive control. The cell-associated fluorescence (Cy5 (+) neurons) for the Cy5 siRNA-LNPs (+ PEG-DMG) group was about 94%—2-fold greater than the neurons transfected with naked Cy5 siRNA group *(Figure 4c, e, and f)*. As expected, despite its transfection-induced toxicity, Cy5 siRNA-Lipofectamine RNAiMAX-treated cells demonstrated the highest proportion of Cy5 (+) cells *(Figure 4c, e, and f)*. On the other hand, cells treated with LNPs appeared healthy and showed no visible signs of toxicity, highlighting the safety of LNPs over cationic transfection agents like Lipofectamine RNAiMAX. There was a

significant difference in the uptake of neurons transfected with naked Cy5 siRNA as compared to the neurons transfected with the LNPs (both with and without PEG-DMG) emphasizing the need for an effective transfection agent for neural cell uptake *(Figure 4f)*.

We also performed fluorescence microscopy to qualitatively study the uptake of Cy5 siRNA into neural cells. A technical caveat of such qualitative assessments is rooted in the fact that the observed/apparent fluorescent intensities are not normalized to cell number. The cells appeared to be healthy, and spindle-shaped in all the treatment groups except for the Lipofectamine RNAiMAX group where cells appeared stressed and rounded as early as at the 2 h timepoint (*Figure 5a)*. As described earlier, we speculate that this is due strong cationic nature of Lipofectamine RNAiMAX. We did not observe a greater uptake for cells treated with LNPs at 100 nM siRNA concentration (*Supplementary Figure 2)*. Nearly all the cells in the field showed Cy5 fluorescent signals 24 h-post exposure (*Figure 5c)* compared to the 2 and 4 h time points (*Figure 5a and b)*, suggesting that neural cells require a longer transfection time compared to non-neural cells. LNPs formulated with PEG-DMG showed a time-dependent increase in the uptake of Cy5 siRNA as opposed to LNPs without PEG-DMG. The time dependent uptake of LNPs formulated with PEG-DMG was in agreement with the PEG-DMG dissociation kinetics as predicted by Mui *et al*. (54). The PEG-lipid component of the LNPs undergoes desorption from the surface of LNPs which results in efficient uptake of the cargo into the cells (55). Studies have reported desorption rates of PEG-DMG from the LNPs at a rate of 45%/h only after which LNPs were taken up by cells (54). We observed a similar trend of Cy5 siRNA uptake when neurons were transfected with LNPs (+ PEG-DMG). At the 2 and 4 h time points, most (but not all) of the cells had efficiently taken up the LNPs. However, 24 h post-treatment, almost all the cells in the field of view showed

fluorescent puncta corresponding to Cy5 siRNA. In contrast, in cells transfected with Cy5 siRNA-LNPs (- PEG-DMG), all the cells demonstrated complete and uniform uptake irrespective of the incubation period. The effects of RNAiMAX-mediated toxicity were evident via altered cell morphology seen in the phase contrast images.

Overall, both flow cytometry and fluorescent microscopy analysis in cortical neurons demonstrated efficient uptake of siRNA delivered using LNPs in the absence of noticeable toxicity while the cationic Lipofectamine RNAiMAX-mediated uptake was concomitant with significant cellular toxicity. Based on these findings, we conclude that LNPs are a safe carrier for siRNA delivery to neural cells. We are currently screening a pre-existing LNP library prepared using different lipidoid chemistries to identify LNP candidates for safe and efficient neuronal gene knockdown. We anticipate that the results of these studies will set the foundation for using LNPs for neural cell transfection in a variety of CNS diseases. While our approach validates using LNPs for uptake of siRNA into neural cells, their knockdown efficacy and therapeutic index remain an open question which we are currently investigating.

Conclusion

SiRNA-loaded LNPs remained stable over a period of seven days and were well-tolerated by neural cell models, allowing their further exploration for gene silencing. Although the LNPs are comparable to Lipofectamine RNAiMAX in facilitating siRNA uptake into cortical neurons, the ionizable cationic LNPs are safer and well-tolerated compared to the cationic Lipofectamine RNAiMAX. PEG-DMG served a crucial role in maintaining lower particle diameters that likely

resulted in efficient uptake into primary rat cortical neurons. Our findings suggest that LNPs hold promise for further silencing of therapeutically-relevant neuronal targets like TRPV1.

Acknowledgements

This work was supported via start-up funds for the Manickam laboratory from Duquesne University (DU) and a 2021 Faculty Development Fund (Office of Research, DU) to the PI. We are grateful to Dr. Kathryn A. Whitehead (Carnegie Mellon University) and her group for their support. We are grateful to Drs. Jane E. Hartung and Michael S. Gold (University of Pittsburgh) for providing the DRG cultures. We express our appreciation to Mr. Duncan Dobbins (Duquesne University) for his assistance with the graphical abstract.

References

1. Wu SY, McMillan NAJ. Lipidic systems for in vivo siRNA delivery. AAPS J. 2009;11(4):639–52.
2. Wang J, Lu Z, Wientjes MG, Au JLS. Delivery of siRNA therapeutics: Barriers and carriers. AAPS J. 2010;12(4):492–503.
3. Akinc A, Maier M, Manoharan M, Fitzgerald K, Jayaraman M, Barros S, et al. The Onpattro story and the clinical translation of nanomedicines containing nucleic acid-based drugs. Nat Nanotechnol. 2019 Dec 1;14:1084–7.
4. Ryan Cross. Without these lipid shells, there would be no mRNA vaccines for COVID-19. Chem Eng News. 2021;16–9.
5. Katakowski JA, Mukherjee G, Wilner SE, Maier KE, Harrison MT, Di Lorenzo TP, et al. Delivery of siRNAs to dendritic cells using DEC205-targeted lipid nanoparticles to inhibit immune responses. Mol Ther. 2016;24(1):146–55.
6. Uemura Y, Naoi T, Kanai Y, Kobayashi K. The efficiency of lipid nanoparticles with an original cationic lipid as a siRNA delivery system for macrophages and dendritic cells. Pharm Dev Technol. 2018 Apr 24;24:1–22.
7. Whitehead KA, Dorkin JR, Vegas AJ, Chang PH, Veiseh O, Matthews J, et al. Degradable lipid nanoparticles with predictable in vivo siRNA delivery activity. Nat Commun. 2014;5.
8. Lopes CDF, Gonçalves NP, Gomes CP, Saraiva MJ, Pêgo AP. BDNF gene delivery mediated by neuron-targeted nanoparticles is neuroprotective in peripheral nerve injury. Biomaterials. 2017;121:83–96.

9. Haney MJ, Klyachko NL, Zhao Y, Gupta R, Plotnikova EG, He Z, et al. Exosomes as drug delivery vehicles for Parkinson's disease therapy. J Control Release [Internet]. 2015;207:18–30. Available from: http://dx.doi.org/10.1016/j.jconrel.2015.03.033
10. Wolfe D, Mata M, Fink DJ. Targeted drug delivery to the peripheral nervous system using gene therapy. Neurosci Lett [Internet]. 2012;527(2):85–9. Available from: http://dx.doi.org/10.1016/j.neulet.2012.04.047
11. H. Ferreira-Vieira T, M. Guimaraes I, R. Silva F, M. Ribeiro F. Alzheimer's disease: Targeting the Cholinergic System. Curr Neuropharmacol. 2016;14(1):101–15.
12. Yang L, Han B, Zhang Z, Wang S, Bai Y, Zhang Y, et al. Extracellular vesicle-mediated delivery of circular RNA SCMH1 promotes functional recovery in rodent and nonhuman primate ischemic stroke models. Circulation. 2020;142(6):556–74.
13. Kim J, Jozic A, Sahay G. Naturally Derived Membrane Lipids Impact Nanoparticle-Based Messenger RNA Delivery. Cell Mol Bioeng. 2020;13(5):463–74.
14. Kulkarni JA, Witzigmann D, Chen S, Cullis PR, Van Der Meel R. Lipid Nanoparticle Technology for Clinical Translation of siRNA Therapeutics. Acc Chem Res. 2019;52(9):2435–44.
15. Rehman ZU, Zuhorn IS, Hoekstra D. How cationic lipids transfer nucleic acids into cells and across cellular membranes: Recent advances. J Control Release [Internet]. 2013;166(1):46–56. Available from: http://dx.doi.org/10.1016/j.jconrel.2012.12.014
16. Soenen SJH, Brisson AR, De Cuyper M. Addressing the problem of cationic lipid-mediated toxicity: The magnetoliposome model. Biomaterials [Internet]. 2009;30(22):3691–701. Available from: http://dx.doi.org/10.1016/j.biomaterials.2009.03.040
17. Dahlman J, Kauffman K, Langer R, Anderson D. Nanotechnology for In vivo Targeted siRNA Delivery. Adv Genet. 2014 Nov 21;88:37–69.
18. Wan C, Allen T, Cullis P. Lipid nanoparticle delivery systems for siRNA-based therapeutics. Drug Deliv Transl Res. 2014 Feb 1;4.
19. Love KT, Mahon KP, Levins CG, Whitehead KA, Querbes W, Dorkin JR, et al. Lipid-like materials for low-dose, in vivo gene silencing. Proc Natl Acad Sci U S A. 2010;107(5):1864–9.
20. Novobrantseva TI, Borodovsky A, Wong J, Klebanov B, Zafari M, Yucius K, et al. Systemic RNAi-mediated gene silencing in nonhuman primate and rodent myeloid cells. Mol Ther - Nucleic Acids. 2012;1(1):e4.
21. Blakney AK, McKay PF, Yus BI, Aldon Y, Shattock RJ. Inside out: optimization of lipid nanoparticle formulations for exterior complexation and in vivo delivery of saRNA. Gene Ther [Internet]. 2019;26(9):363–72. Available from: http://dx.doi.org/10.1038/s41434-019-0095-2
22. Naseri N, Valizadeh H, Zakeri-Milani P. Solid lipid nanoparticles and nanostructured lipid carriers: Structure preparation and application. Adv Pharm Bull [Internet]. 2015;5(3):305–13. Available from: http://dx.doi.org/10.15171/apb.2015.043
23. Cullis PR, Hope MJ. Lipid Nanoparticle Systems for Enabling Gene Therapies. Mol Ther [Internet]. 2017;25(7):1467–75. Available from: http://dx.doi.org/10.1016/j.ymthe.2017.03.013
24. J. Jones L, T. Yue S, Cheung Ching-Ying, L. Singer V. RNA Quantitation by Fluorescence-Based Solution Assay- RiboGreen Reagent Characterization.pdf. Anal Biochem [Internet]. 1998;374(265):368–74. Available from: http://files/191/J. Jones et al.

- 1998 - RNA Quantitation by Fluorescence-Based Solution As.pdf
25. Hartung JE, Gold MS. GCaMP as an indirect measure of electrical activity in rat trigeminal ganglion neurons. Cell Calcium [Internet]. 2020;89(April):102225. Available from: https://doi.org/10.1016/j.ceca.2020.102225
26. Dave KM, Ali L, Manickam DS. Characterization of the SIM-A9 cell line as a model of activated microglia in the context of neuropathic pain. PLoS One [Internet]. 2020;15(4):1–28. Available from: http://dx.doi.org/10.1371/journal.pone.0231597
27. Dave KM, Han L, Jackson MA, Kadlecik L, Duvall CL, S Manickam D. DNA Polyplexes of a Phosphorylcholine-Based Zwitterionic Polymer for Gene Delivery. Pharm Res. 2020;37(9).
28. Dave KM, Zhao W, Hoover C, D'Souza A, S Manickam D. Extracellular Vesicles Derived from a Human Brain Endothelial Cell Line Increase Cellular ATP Levels. AAPS PharmSciTech. 2021;22(1).
29. Honary S, Zahir F. Effect of zeta potential on the properties of nano-drug delivery systems - A review (Part 1). Trop J Pharm Res. 2013;12(2):255–64.
30. Ing LY, Zin NM, Sarwar A, Katas H. Antifungal activity of chitosan nanoparticles and correlation with their physical properties. Int J Biomater. 2012;2012.
31. Li X, Sloat BR, Yanasarn N, Cui Z. Relationship between the size of nanoparticles and their adjuvant activity: Data from a study with an improved experimental design. Eur J Pharm Biopharm. 2011;78(1):107–16.
32. Breznan D, Das DD, Mackinnon-Roy C, Bernatchez S, Sayari A, Hill M, et al. Physicochemical Properties Can Be Key Determinants of Mesoporous Silica Nanoparticle Potency in Vitro. ACS Nano. 2018;12(12):12062–79.
33. Shin SW, Song IH, Um SH. Role of physicochemical properties in nanoparticle toxicity. Nanomaterials. 2015;5(3):1351–65.
34. Navya PN, Daima HK. Rational engineering of physicochemical properties of nanomaterials for biomedical applications with nanotoxicological perspectives. Nano Converg. 2016;3(1):1–14.
35. Braakhuis HM, Park MVDZ, Gosens I, De Jong WH, Cassee FR. Physicochemical characteristics of nanomaterials that affect pulmonary inflammation. Part Fibre Toxicol. 2014;11(1).
36. Witzigmann D, Kulkarni JA, Leung J, Chen S, Cullis PR, Meel R Van Der. Since January 2020 Elsevier has created a COVID-19 resource centre with free information in English and Mandarin on the novel coronavirus COVID- 19 . The COVID-19 resource centre is hosted on Elsevier Connect , the company ' s public news and information . 2020;(January).
37. Chen S, Tam YYC, Lin PJC, Leung AKK, Tam YK, Cullis PR. Development of lipid nanoparticle formulations of siRNA for hepatocyte gene silencing following subcutaneous administration. J Control Release [Internet]. 2014;196:106–12. Available from: http://dx.doi.org/10.1016/j.jconrel.2014.09.025
38. Romberg B, Hennink WE, Storm G. Sheddable coatings for long-circulating nanoparticles. Pharm Res. 2008;25(1):55–71.
39. Kulkarni JA, Darjuan MM, Mercer JE, Chen S, Van Der Meel R, Thewalt JL, et al. On the Formation and Morphology of Lipid Nanoparticles Containing Ionizable Cationic Lipids and siRNA. ACS Nano. 2018;12(5):4787–95.
40. Pecze L, Jósvay K, Blum W, Petrovics G, Vizler C, Oláh Z, et al. Activation of

endogenous TRPV1 fails to induce overstimulation-based cytotoxicity in breast and prostate cancer cells but not in pain-sensing neurons. Biochim Biophys Acta - Mol Cell Res [Internet]. 2016;1863(8):2054–64. Available from: http://dx.doi.org/10.1016/j.bbamcr.2016.05.007

41. Esposito MF, Malayil R, Hanes M, Deer T. Unique Characteristics of the Dorsal Root Ganglion as a Target for Neuromodulation. Pain Med (United States). 2019;20:S23–30.

42. Yu X, Liu H, Hamel KA, Morvan MG, Yu S, Leff J, et al. Dorsal root ganglion macrophages contribute to both the initiation and persistence of neuropathic pain. Nat Commun [Internet]. 2020;11(1):1–12. Available from: http://dx.doi.org/10.1038/s41467-019-13839-2

43. Xu Q, Zhang XM, Duan KZ, Gu XY, Han M, Liu BL, et al. Peripheral tgf-β1 signaling is a critical event in bone cancer-induced hyperalgesia in rodents. J Neurosci. 2013;33(49):19099–111.

44. Davey HM, Kell DB. Flow cytometry and cell sorting of heterogeneous microbial populations: The importance of single-cell analyses. Microbiol Rev. 1996;60(4):641–96.

45. BIO-RAD. Flow Cytometry Data Analysis [Internet]. Available from: https://www.bio-rad-antibodies.com/flow-cytometry-gating-strategies.html?JSESSIONID_STERLING=1C53AF8B8470DB1019FE94619BC4BF4F.ecommerce1&evCntryLang=US-en&cntry=US&thirdPartyCookieEnabled=true&wdLOR=cBC762A28-80AB-9C4A-8B9C-0FF8F79509C6

46. Ryals RC, Patel S, Acosta C, McKinney M, Pennesi ME, Sahay G. The effects of PEGylation on LNP based mRNA delivery to the eye. PLoS One [Internet]. 2020;15(10 October):1–17. Available from: http://dx.doi.org/10.1371/journal.pone.0241006

47. Chen S, Tam YYC, Lin PJC, Sung MMH, Tam YK, Cullis PR. Influence of particle size on the in vivo potency of lipid nanoparticle formulations of siRNA. J Control Release [Internet]. 2016;235:236–44. Available from: http://dx.doi.org/10.1016/j.jconrel.2016.05.059

48. van der Meel R, Chen S, Zaifman J, Kulkarni J, Zhang XR, Tam Y, et al. Modular lipid nanoparticle platform technology for siRNA and lipophilic prodrug delivery. bioRxiv. 2020;(2020).

49. Buyens K, Lucas B, Raemdonck K, Braeckmans K, Vercammen J, Hendrix J, et al. A fast and sensitive method for measuring the integrity of siRNA-carrier complexes in full human serum. J Control Release. 2008;126(1):67–76.

50. Walsh C, Ou K, Belliveau N, Leaver T, Wild A, Huft J, et al. Microfluidic-Based Manufacture of siRNA-Lipid Nanoparticles for Therapeutic Applications. Methods Mol Biol. 2014 Feb 25;1141:109–20.

51. Ball R, Bajaj P, Whitehead KA. Achieving long-term stability of lipid nanoparticles: Examining the effect of pH, temperature, and lyophilization. Int J Nanomedicine. 2017;12:305–15.

52. Howard KA, Rahbek UL, Liu X, Damgaard CK, Glud SZ, Andersen M, et al. RNA Interference in Vitro and in Vivo Using a Novel Chitosan/siRNA Nanoparticle System. Mol Ther [Internet]. 2006;14(4):476–84. Available from: http://dx.doi.org/10.1016/j.ymthe.2006.04.010

53. Thiramanas R, Li M, Jiang S, Landfester K, Mailänder V. Cellular Uptake of siRNA-Loaded Nanocarriers to Knockdown PD-L1: Strategies to Improve T-cell Functions. Cells.

2020;9(9):1–12.
54. Mui BL, Ying K Tam , Muthusamy Jayaraman , Steven M Ansell, Xinyao Du, Yuen Yi C Tam PJL, Chen S, Narayanannair JK, Kallanthottathil G Rajeev, Muthiah Manoharan, Akin Akinc, Martin A Maier PC, Madden TD, et al. Influence of Polyethylene Glycol Lipid Desorption Rates on Pharmacokinetics and Pharmacodynamics of siRNA Lipid Nanoparticles. Mol Ther - Nucleic Acids. 2013;2(12):1–8.
55. Kulkarni JA, Cullis PR, Van Der Meel R. Lipid Nanoparticles Enabling Gene Therapies: From Concepts to Clinical Utility. Nucleic Acid Ther. 2018;28(3):146–57.

Lipidoid nanoparticles increase siRNA uptake into neuronal cells

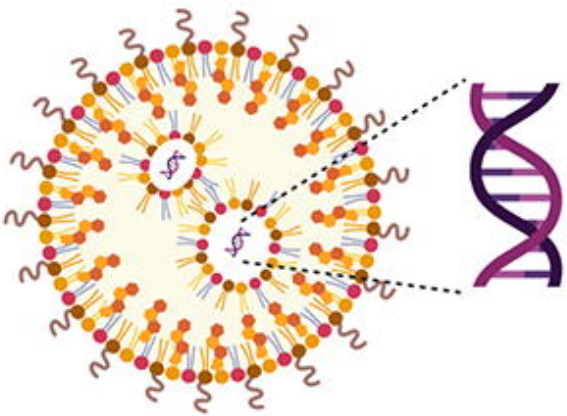

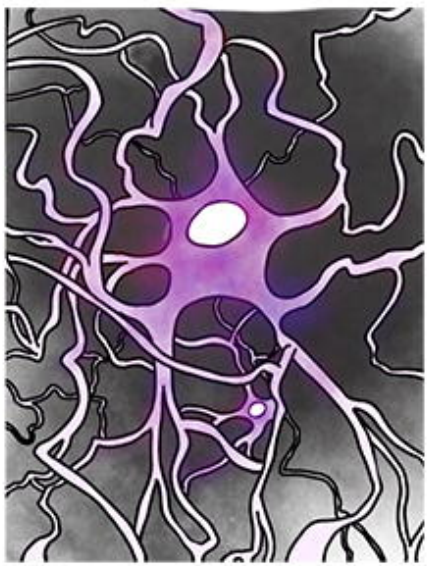

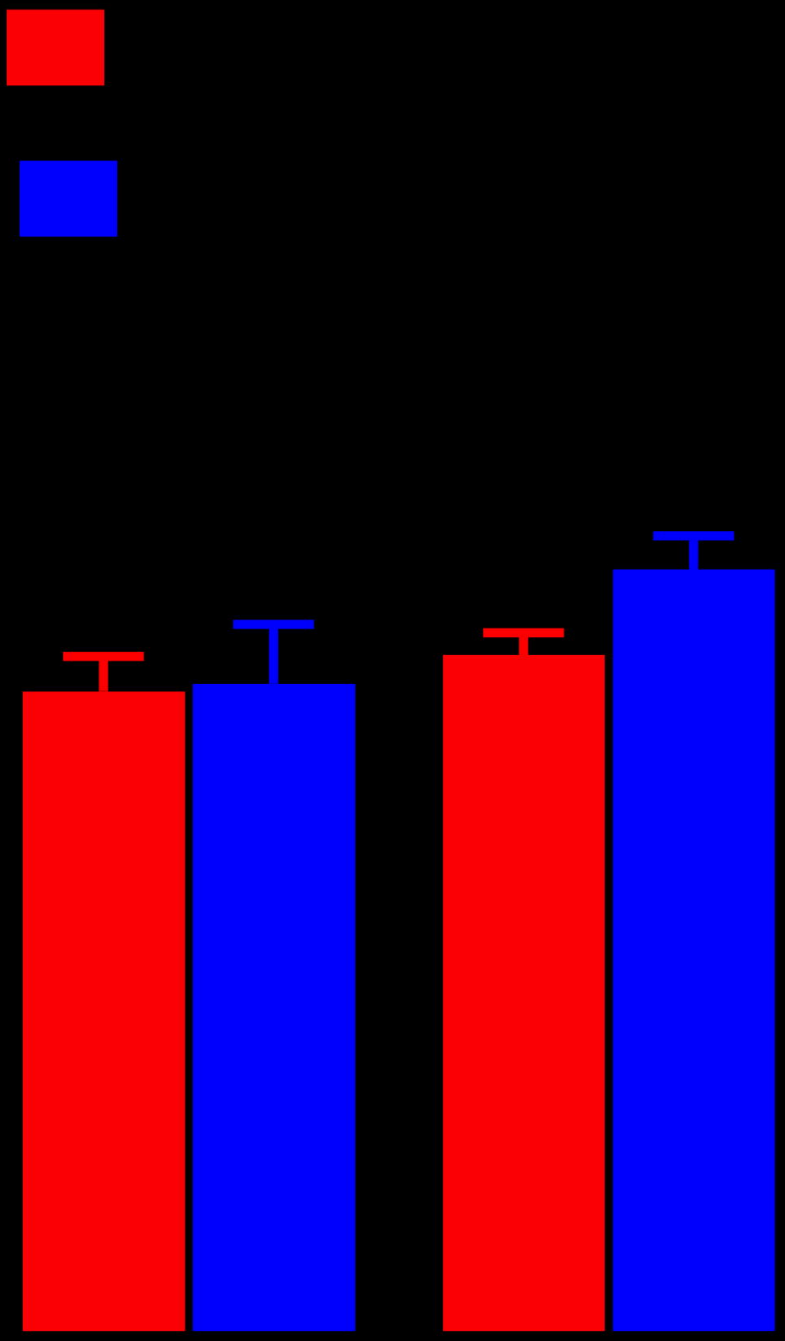

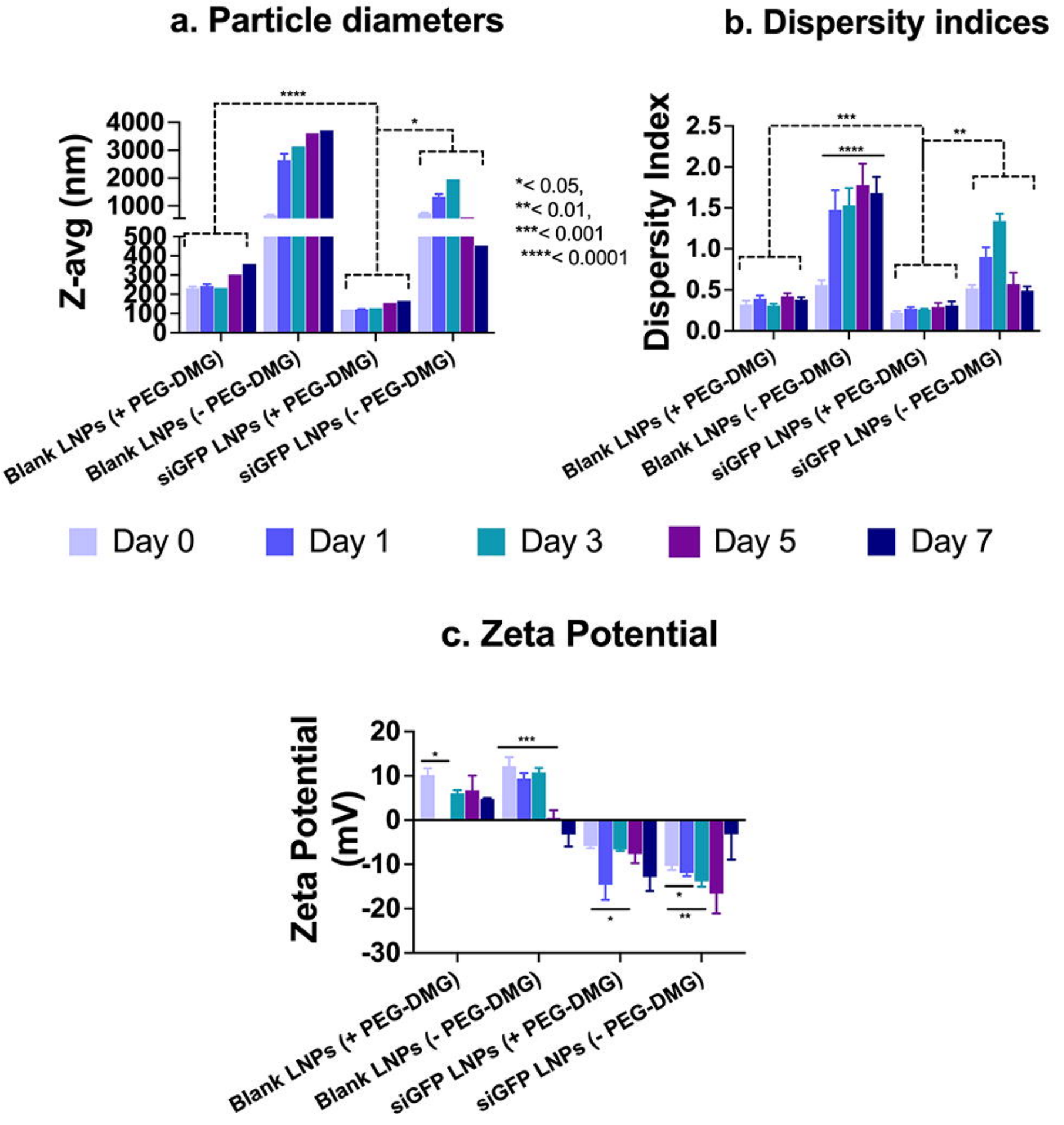
a. Particle diameters
b. Dispersity indices
Z-avg (nm)
4000
3000
2000
1000
500
400
300
200
100
0
****
*
*< 0.05,
**< 0.01,
***< 0.001
****< 0.0001
Dispersity Index
2.5
2.0
1.5
1.0
0.5
0.0
***
****
**
Blank LNPs (+ PEG-DMG)
Blank LNPs (- PEG-DMG)
siGFP LNPs (+ PEG-DMG)
siGFP LNPs (- PEG-DMG)
Day 0
Day 1
Day 3
Day 5
Day 7
c. Zeta Potential
Zeta Potential (mV)
20
10
0
-10
-20
-30
*
***
*
*
**

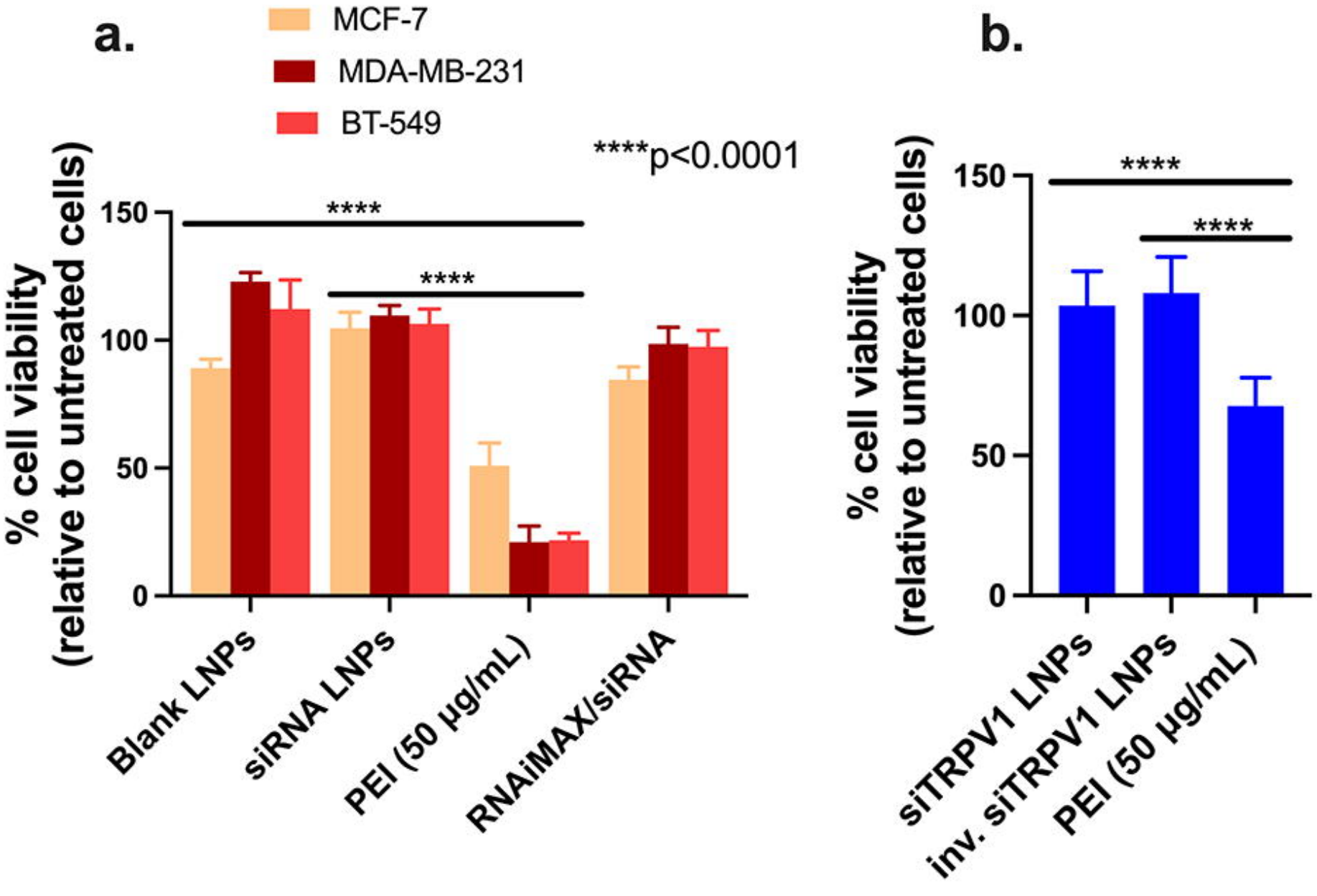
a.
MCF-7
MDA-MB-231
BT-549
****p<0.0001
% cell viability
(relative to untreated cells)
150
100
50
0
****
****
Blank LNPs
siRNA LNPs
PEI (50 µg/mL)
RNAiMAX/siRNA
b.
% cell viability
(relative to untreated cells)
150
100
50
0
****
****
siTRPV1 LNPs
inv. siTRPV1 LNPs
PEI (50 µg/mL)

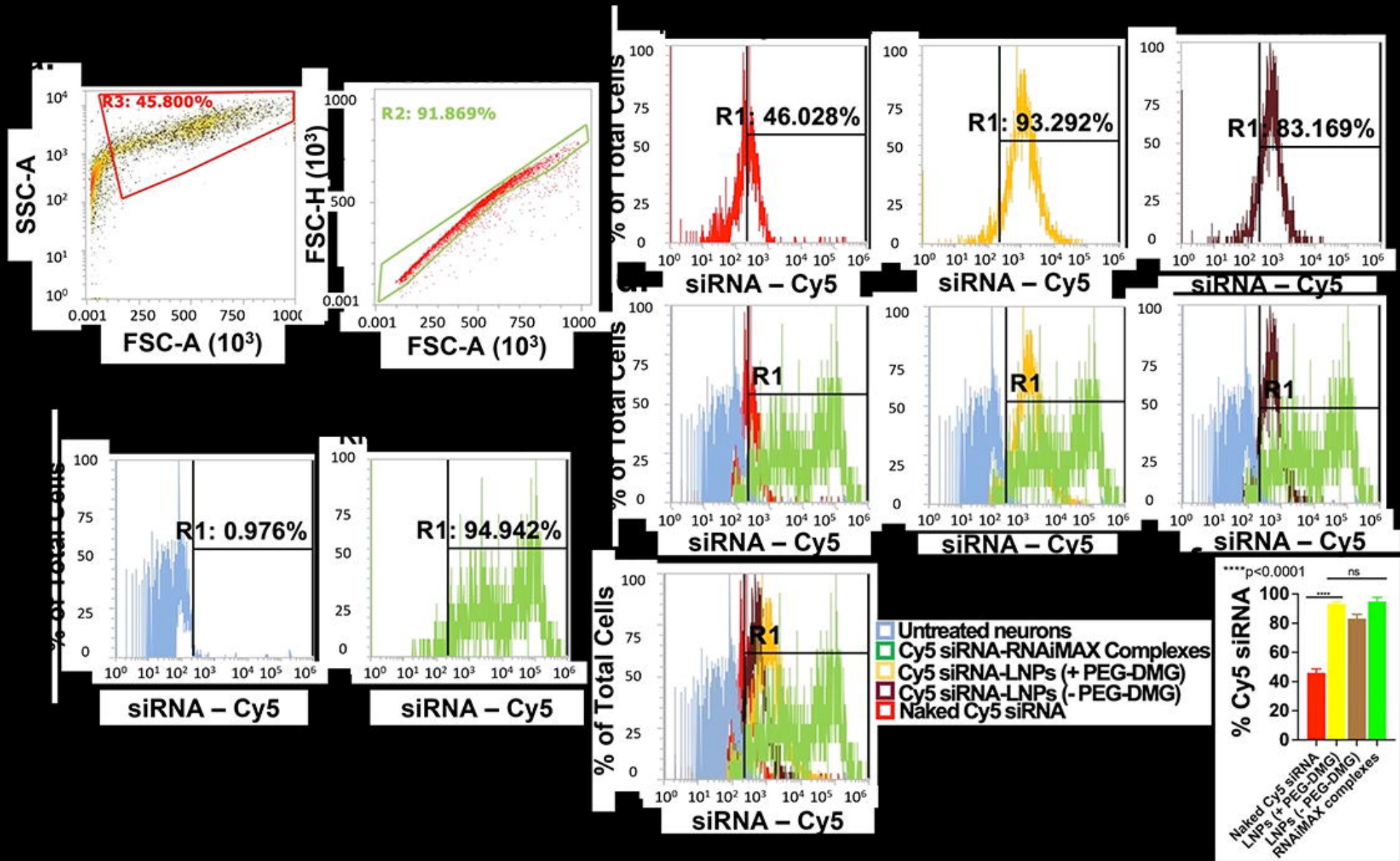
R3: 45.800%
SSC-A
FSC-A (10³)
R2: 91.869%
FSC-H (10³)
FSC-A (10³)
R1: 46.028%
R1: 93.292%
R1: 83.169%
R1: 0.976%
R1: 94.942%
R1
% of Total Cells
siRNA – Cy5
Untreated neurons
Cy5 siRNA-RNAiMAX Complexes
Cy5 siRNA-LNPs (+ PEG-DMG)
Cy5 siRNA-LNPs (- PEG-DMG)
Naked Cy5 siRNA
****p<0.0001
ns
% Cy5 siRNA
Naked Cy5 siRNA
LNPs (+ PEG-DMG)
LNPs (- PEG-DMG)
RNAiMAX complexes

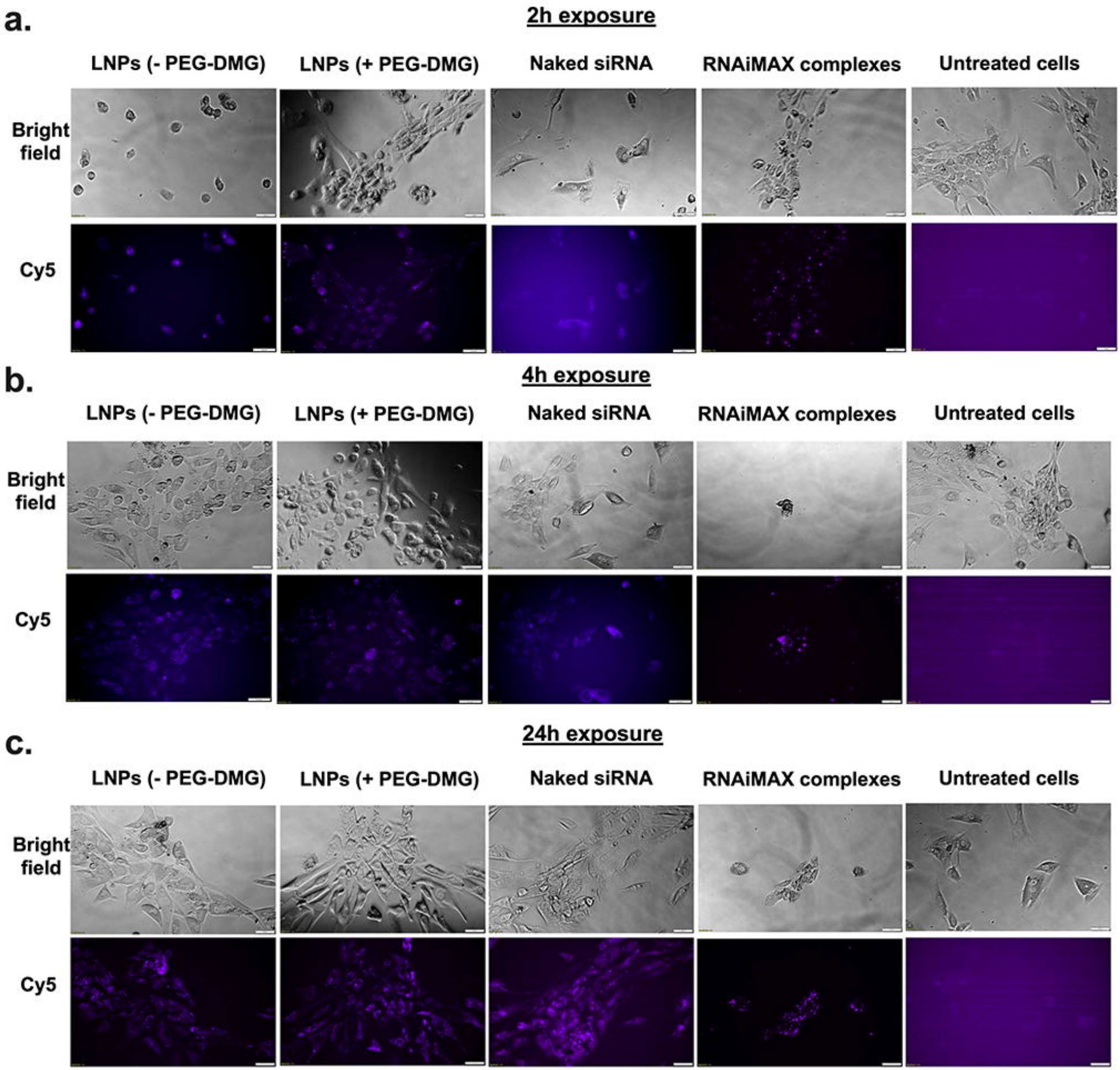
a.
2h exposure
LNPs (- PEG-DMG)
LNPs (+ PEG-DMG)
Naked siRNA
RNAiMAX complexes
Untreated cells
Bright field
Cy5
b.
4h exposure
LNPs (- PEG-DMG)
LNPs (+ PEG-DMG)
Naked siRNA
RNAiMAX complexes
Untreated cells
Bright field
Cy5
c.
24h exposure
LNPs (- PEG-DMG)
LNPs (+ PEG-DMG)
Naked siRNA
RNAiMAX complexes
Untreated cells
Bright field
Cy5

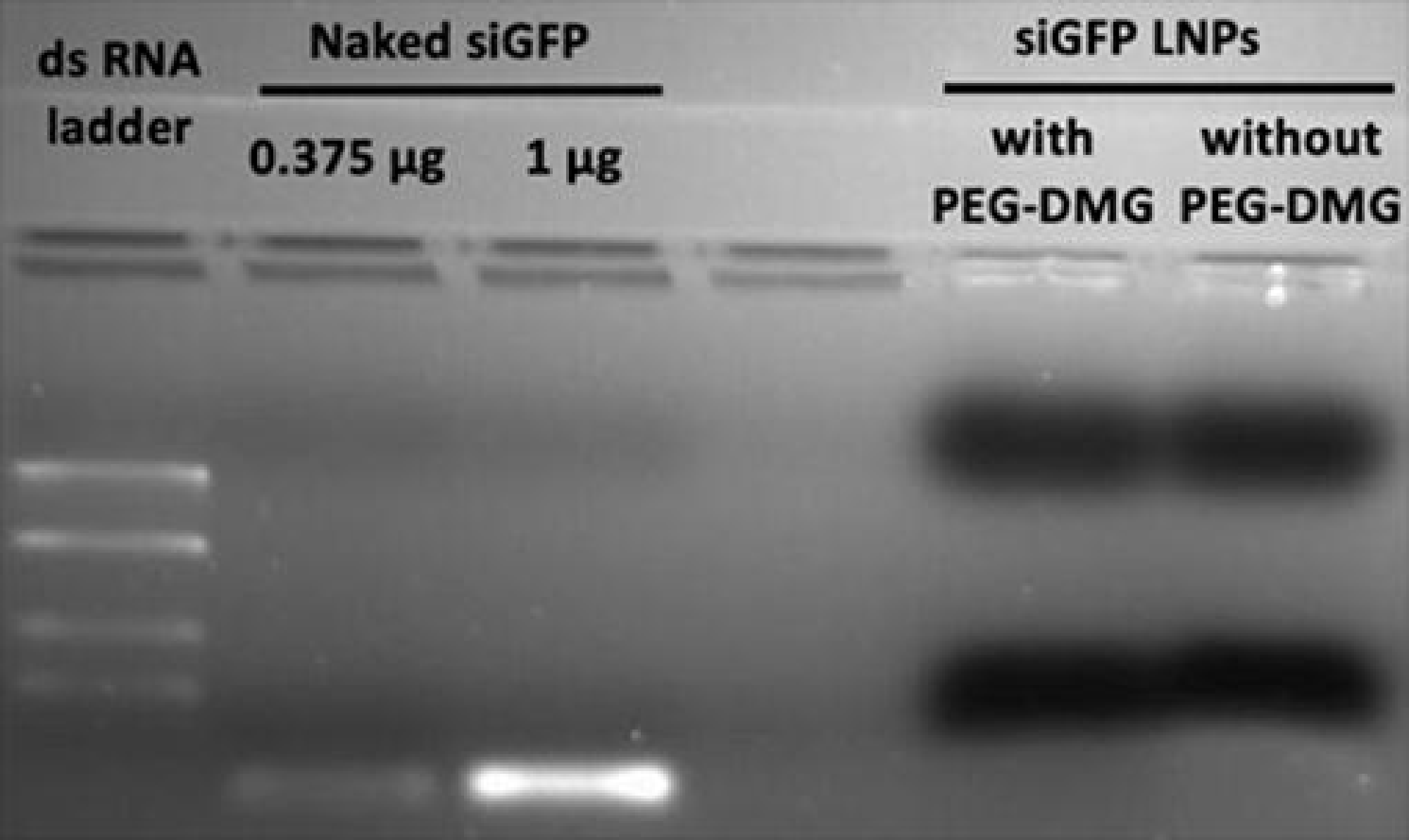
ds RNA ladder
Naked siGFP
0.375 µg
1 µg
siGFP LNPs
with PEG-DMG
without PEG-DMG

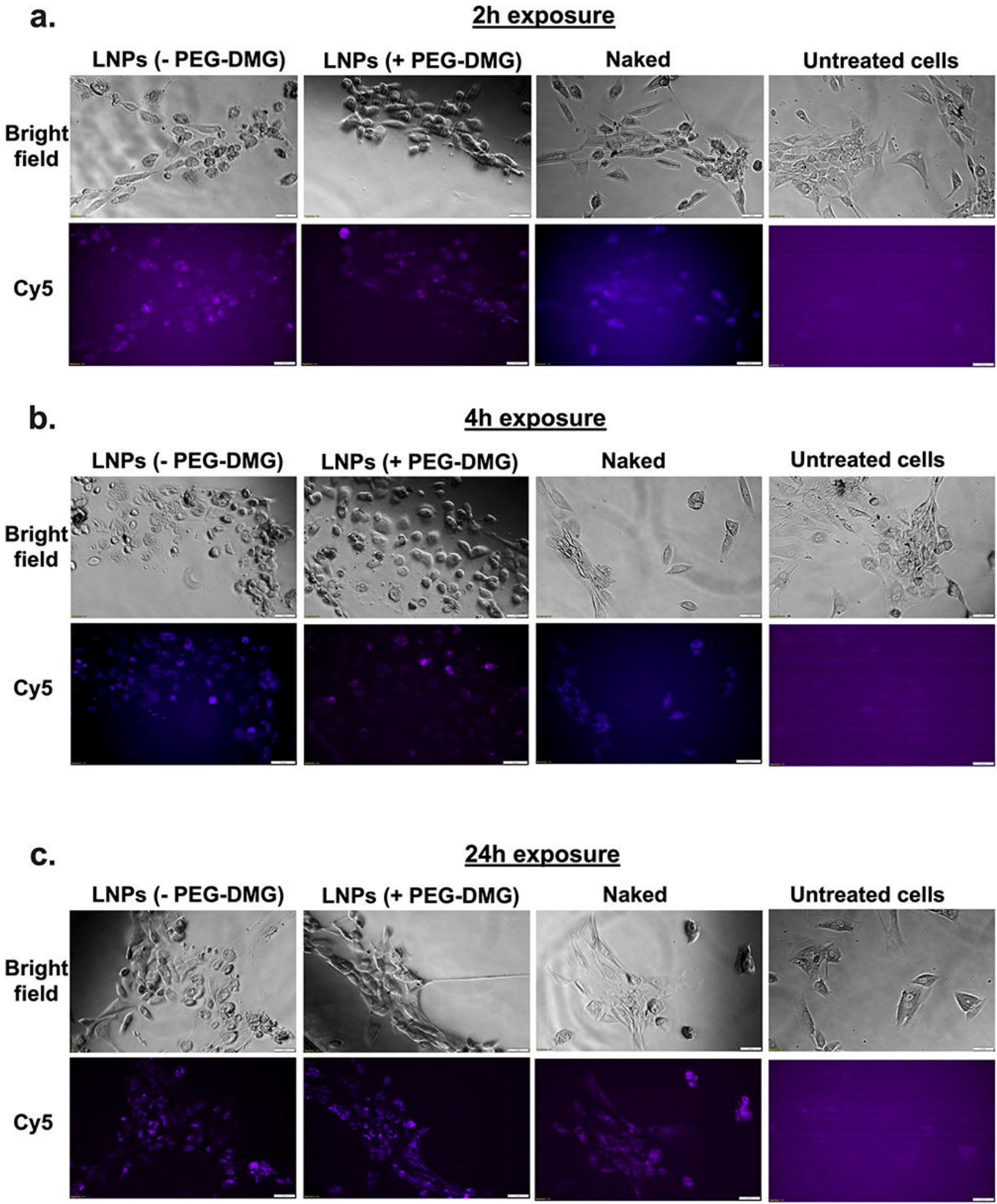
a.
2h exposure
LNPs (- PEG-DMG)
LNPs (+ PEG-DMG)
Naked
Untreated cells
Bright field
Cy5
b.
4h exposure
LNPs (- PEG-DMG)
LNPs (+ PEG-DMG)
Naked
Untreated cells
Bright field
Cy5
c.
24h exposure
LNPs (- PEG-DMG)
LNPs (+ PEG-DMG)
Naked
Untreated cells
Bright field
Cy5